Available online at www.sciencedirect.com
SCIENCE DIRECT®

Talanta 65 (2005) 1143–1148

Talanta

www.elsevier.com/locate/talanta

Study of adsorption of methylene blue and new methylene blue in liquid–solid interface by slab optical waveguide spectroscopy

Li-Xian Sun[a,b,*], Naoki Matsuda[a,*], Akiko Takatsu[c], Kenji Kato[c], Tatsuhiro Okada[d]

[a] *Nanoarchitectonics Research Center, National Institute of Advanced Industrial Science and Technology, Tsukuba 305-8565, Japan*
[b] *Dalian Institute of Chemical Physics, Chinese Academy of Sciences, 116023 Dalian, PR China*
[c] *National Metrological Laboratory, National Institute of Advanced Industrial Science and Technology, Tsukuba 305-8565, Japan*
[d] *National Institute of Advanced Industrial Science and Technology, Tsukuba 305-8565, Japan*

Received 30 November 2003; received in revised form 5 May 2004; accepted 10 June 2004
Available online 23 November 2004

Abstract

A slab optical waveguide (SOWG) has been used for study of adsorption of both methylene blue (MB) and new methylene blue (NMB) in liquid–solid interface. Adsorption characteristics of MB and NMB on both bare SOWG and silanized SOWG by octadecyltrichlorosilane (ODS) were compared. Effect of pH on adsorption on MB and NMB was investigated. Binding rate constant analysis showed that both MB and NMB on bare SOWG demonstrates larger association constants than those on ODS-SOWG. Interactions of MB and NMB on bare SOWG and ODS-SOWG were analyzed by molecular mechanics calculation method. The binding energy change was in the following order: $E_{\text{NMB–bare}} > E_{\text{MB–bare}} > E_{\text{NMB–ODS}} > E_{\text{MB–ODS}}$.

Keywords: Adsorption; Methylene blue; New methylene blue; Slab optical waveguide spectroscopy; Octadecyltrichlorosilane

---

1. Introduction

Dyes have been found widely applications in many fields so far. For example, they are usually utilized as electrocatalysts for biochemical sensors [1,2], sensitizers in solar energy conversion cells [3–5], food colorants [6], pharmaceutical ingredient [7], coloring agent for textiles and so on. The photoelectric transfer efficiency in the solar cells with respect to wavelength of irradiated light is related to the adsorbed states and absorption spectra of the dye molecules. It plays an important role to get in situ information about the adsorbed states and structure of the dye molecules adsorbed on electrode/electrolyte interfaces in order to develop and improve performance of solar cells. However, it is difficult to realize in situ observation about the adsorbed dye, as the amount of dye molecules at the interface is much lower than those in the bulk in many cases. Furthermore, what we think is that new dye mixture system may get much better performance of solar cell than one dye system. On the other hand, it is very difficult to clean the manufacturing equipment where the dyes are used as raw materials, due to the high adsorption affinity of the dyes. The removal of the adsorbed dyes from the equipment walls or container wall like glass beaker usually needs a lot of water, detergents and energy. Therefore, it is very important to study the adsorption characteristics of dyes in liquid–solid surface in order to clean the equipment surface and container wall. The aggregation of dyes has been observed as a general phenomenon in the solid state, in LB films and in solutions.

A slab optical waveguide (SOWG) is very important for integrated optics. It has been intensively applied to optical sensing of surface chemical species and chemical reactions

---

* Corresponding authors. Tel.: +86 411 4379213 (L.-X. Sun)/+81 298 61 4637 (N. Matsuda); fax: +86 411 4379213 (L.-X. Sun)/+81 298 61 4637 (N. Matsuda).
E-mail addresses: lxsun@dicp.ac.cn (L.-X. Sun), naoki.matsuda@aist.go.jp (N. Matsuda).

0039-9140/$ – see front matter © 2004 Elsevier B.V. All rights reserved.
doi:10.1016/j.talanta.2004.06.047

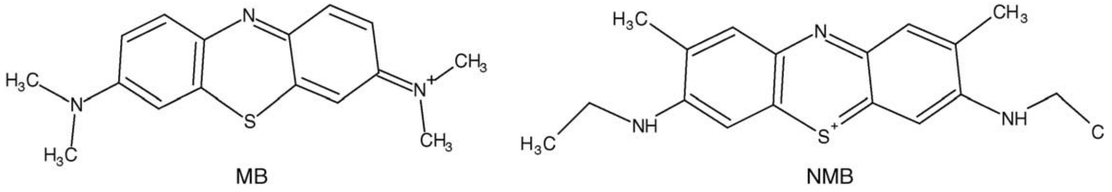

Fig. 1. Structures of methylene blue (MB) and new methylene blue (NMB).

[8–10]. The application of the SOWG for analysis of chemical systems was first proposed by Midwinter [11]. According to Midwinter's idea [11], thin film waveguides could be employed as internal reflection elements in attenuated total reflection (ATR) spectroscopy. As compared with conventional transmission technology like UV–visible spectrophotometry, the ATR allows measurement to be performed in highly scattering liquids, and has higher sensitivity, for instance, the absorption spectra of adsorbed materials were observed to determine the adsorbed species on solid–liquid interfaces with even below a monolayer coverage. Recently, a number of publications have reviewed analytical application of SOWG [12,13].

We have studied adsorption characteristics of cytochrome *C*, hemoglobin, etc. on a liquid–solid interface with novel SOWG technique developed by our laboratory [14–27]. Recently, present authors also studied quantitative determination of dyes by SOWG and artificial neural network [28]. Methylene blue (MB) and new methylene blue (NMB), as typical phenothiazin days, have been used as redox mediators for biochemical sensors [1,2], etc. In this study, the adsorption of both methylene blue and new methylene blue dyes on liquid–solid interface was investigated by slab optical waveguide.

2. Experimental

2.1. Materials

The chemical structures of MB and NMB are shown in Fig. 1. Toluene and MB were purchased from Kanto Chemical Co., Inc. NMB was obtained from Aldrich (USA). Octadecyltrichlorosilane (ODS) was from Shinetsu Silicon Chemical Co., Inc. non-fluorescent slide glass (Matsunami S-3314, 26 mm (width) × 76 mm (length) × 1 mm (height)) was obtained from Matsunami Glass Ind., Ltd.

The bare SOWG plate for transmitting the light was prepared by ion-exchange process from a non-fluorescent slide glass (Matsunami S-3314, 26 mm (width) × 76 mm (length) × 1 mm (height)) in melted potassium nitrate solution at 400 °C for 60 min. A thin surface layer on the slide glass has been formed after ion exchange. This thin layer has a little higher refractive index as compared with the substrate, and will serve as the core for transmitting the light.

The bare SOWG plate for transmitting the light was prepared by ion-exchange process from a non-fluorescent slide glass (Matsunami S-3314, 26 mm (width) × 76 mm (length) × 1 mm (height)) in melted potassium nitrate solution at 400 °C for 60 min. A thin surface layer on the slide glass has been formed after ion exchange. This thin layer has a slightly higher refractive index as compared with the substrate, and will be used as the core for transmitting the light.

The silanization of the bare plate was carried out with similar procedure proposed by Kingston and Gerhart [29]. Firstly, the bare plate was dipped into 1% octadecylsilane (ODS) in toluene solution for 60 min. Then the plate was fully rinsed with sonication in ethanol, and subsequently washed in pure water so that the loosely adsorbed layers can be removed. Finally the plate was dried in oven at 110 °C for 1 h. Pure water prepared by Milli-Q system (Millipore, Japan) was used throughout.

2.2. Apparatus

The schematic diagram of SOWG apparatus is shown in Fig. 2. It is very similar to that used in our previous study [15]. A Teflon block with a silicon rubber spacer was used as a cell, which was mounted to the SOWG plate by screws. Sample, water and ethanol were pumped into the cell. In this work, a static cell whose dimension is 20 mm in length, 6 mm in width and 10 mm in height was used. A xenon lamp (150 W) was used as excitation source. Light from 380 to 800 nm can be transmitted through the SOWG simultaneously.

The conventional UV–visible spectrophotometric approach was also used for the measurement of spectra of both MB and NMB. The UV–visible spectra of MB and NMB

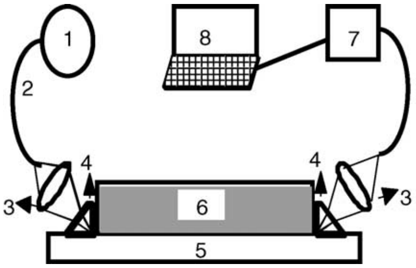

Fig. 2. Schematic diagram of the slab optical waveguide (SOWG) measurement system: 1, Xe lamp; 2, fiber; 3, micro-lense; 4, prism; 5, SOWG; 6, sample cell; 7, CCD; 8, PC computer.

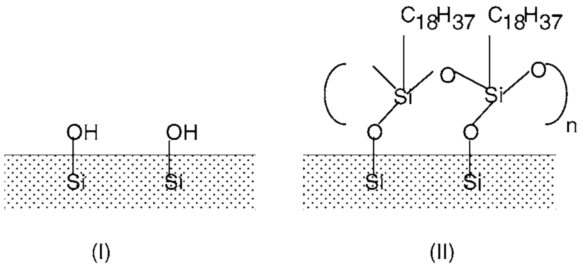

Fig. 3. Schematic structure of both bare SOWG and ODS-SOWG.

solutions were measured with a UV-2100PC (Shimadzu, Japan). The length of the cell is 10 mm. All MB and NMB samples were newly prepared, and diluted from a 1.0 mM stock solution prior to the measurement.

2.3. Molecular mechanics calculations

The binding energies [30,31] between dye molecules and bare SOWG and ODS-SOWG were calculated by molecular mechanics method by using CAChe (Version 3.9, Oxford Molecular Ltd.). All geometric parameters including bond angles, dihedral angles, etc., were optimized without any specific assumptions by conjugate gradient algorithm and MM2 parameters as force field parameters. The energy of the final optimal structure with CAChe is the sum of the following terms: bond stretch, bond angle, bond stretch bend, dihedral angle, improper torsion, van der Waals, electrostatics, hydrogen bond.

2.4. Peak resolution

The dimer peak and monomer peak in spectra for MB and NMB obtained from UV–visible spectrophotometry and SOWG technique were resolved by GRAMS/32 (Galactic Industries Corporation, http://www.galactic.com/).

3. Results and discussion

3.1. Binding energy analysis

Binding energy analysis has been used for molecular recognition study [32] and study of interaction between Nafion film and organic gas [33]. The structure of both bare SOWG and ODS-SOWG can be simply represented in (I) and (II), respectively (Fig. 3) as suggested by Sagiv [34]. For the simplicity of molecular mechanics calculations, the interaction between one segment of SOWG (for bare SOWG, one SiOH segment was taken into account; for ODS-SOWG, $n = 1$) and dye molecules is considered in this study. Suppose one mole segment of SOWG can bind one mole of dye molecule, i.e. they form 1:1 complex. In general cases, however, SOWG–dye complex would not be 1:1, but here the interactions for various dye molecules are compared for 1:1 complex in relative scale. According to reference [32], the binding energy (DetE) is defined as the difference between the most stable energy of $E_{\text{SOWG–dye}}$ complex and the sum of the most stable energies of E_{SOWG} and E_{dye},

$$\text{DetE} = E_{\text{SOWG–dye}} - (E_{\text{SOWG}} + E_{\text{dye}}) \qquad (1)$$

where E_{SOWG}, E_{dye} and $E_{\text{SOWG–dye}}$ were obtained from molecular mechanics calculation with CAChe software as mentioned in Section 2.3 [30,31].

The binding energy of $E_{\text{SOWG–dye}}$ complex is summarized in the second column of Table 1. Table 1 shows that the binding energy change was in the following order: $E_{\text{NMB–bare}} > E_{\text{MB–bare}} > E_{\text{NMB–ODS}} > E_{\text{MB–ODS}}$. This means that the binding energy for both MB and NMB on bare SOWG is larger than that on ODS-SOWG. There can be one possible reason to explain these phenomena. The adsorption sites of glass surface decrease with the ODS modification due to increasing hydrophobicity. One also noticed that the binding energy for NMB on both bare SOWG and ODS-SOWG is larger than that for MB, perhaps due to their different molecular structures.

3.2. Kinetics

Askin Inel and Turk [35] and Haimour and Syed [36] have studied adsorption of dyes on some silicates and olive seeds by using Langmuirian adsorption model. Therefore, one supposes the binding process between dyes (MB and NMB) and bare SOWG/ODS-SOWG

$$\text{SOWG} + \text{dye} \overset{k_1}{\underset{k_2}{\Leftrightarrow}} \text{SOWG–dye} \qquad (2)$$

obeys Langmuir model, where k_1 and k_2 are binding constant and dissociation constant, respectively. Then the kinetics control model under Langmuirian adsorption conditions can be expressed as [32]

Table 1
Comparison of binding energy change and kinetic parameters for binding of MB and NMB on bare SOWG and ODS-SOWG

Binding species	Binding energy, DetE (kcal/mol)	Binding constant, k_1 ($\text{M}^{-1}\,\text{s}^{-1}$)	Dissociation constant, k_2 ($10^{-3}\,\text{s}^{-1}$)	Association constant, K (10^{7})
NMB–ODS-SOWG	−10.59	2560	0.1	2.56
NMB–bare SOWG	−58.35	1520	0.05	3.04
MB–ODS-SOWG	−2.53	1280	0.8	0.16
MB–bare SOWG	−20.80	3680	0.3	1.23

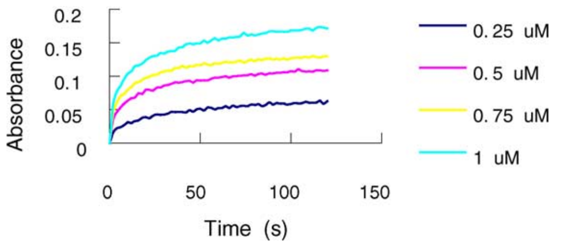

Fig. 4. Time-dependence absorption spectra of MB on ODS-SOWG in a static cell.

$$\Gamma_t = \Gamma_e \left[1 - \exp\left(-\frac{t}{\tau}\right)\right] \tag{3}$$

It can be converted into,

$$\frac{t}{\tau} = \ln\left[\frac{\Gamma_e}{\Gamma_e - \Gamma_t}\right] \tag{4}$$

where Γ_t is the surface concentration of the adsorbate at time t, Γ_e the equilibrium surface concentration at a given bulk concentration C, and τ the relaxation time. According to Lambert–Beer's law, Eq. (4) can be converted into the following equation:

$$\ln\left[\frac{A_e}{A_e - A_t}\right] = \frac{t}{\tau} \tag{5}$$

$$\tau^{-1} = k_1[\text{dye}] + k_2 \tag{6}$$

A_e and A_t correspond to the absorbance at adsorption equilibrium and at time t, respectively. The association constant K is defined as the ratio between k_1 and k_2, i.e. $K = k_1/k_2$. The time dependences of absorbance spectra of MB on ODS-SOWG at four different concentrations are shown in Fig. 4.

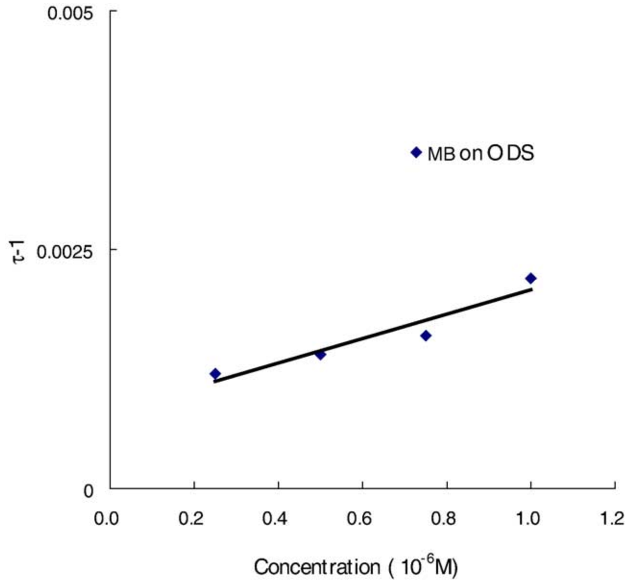

Fig. 5. Plot of τ^{-1} vs. concentration for MB on ODS-SOWG.

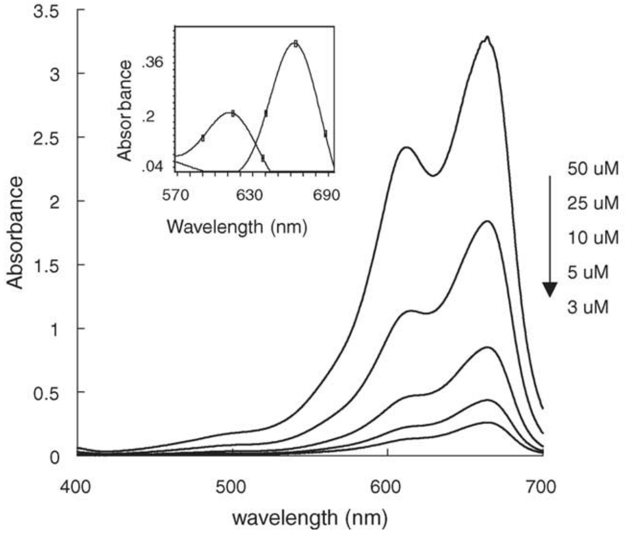

Fig. 6. UV–visible spectra of MB at different concentrations in 1.0 cm light path length cell; the inset exhibits the monomer and dimer spectra of MB after resolution.

The plot of τ^{-1} versus concentration for MB on ODS-SOWG is shown in Fig. 5. The values of k_1, k_2 and K are calculated according to Eq. (6), and summarized in the columns 3–5 of Table 1. The association constant K was in the following order: $K_{\text{NMB–bare}} > K_{\text{NMB–ODS}} > K_{\text{MB–bare}} > K_{\text{MB–ODS}}$ as shown in Table 1. It is in good coincidence with the order of binding energy, except MB on bare SOWG. As mentioned in Section 3.1, the binding energy change is in the following order: $E_{\text{NMB–bare}} > E_{\text{MB–bare}} > \text{E}_{\text{NMB–ODS}} > E_{\text{MB–ODS}}$. Table 1 also indicates that the association constant K for both MB and NMB on bare SOWG is larger than that on ODS-SOWG. If one compares the relationship of binding energy and association constant K for MB and NMB, it seems that NMB on bare/ODS-SOWG has higher binding energy than MB on bare/ODS-SOWG. Therefore, Table 1 shows that NMB on bare/ODS-SOWG gives corresponding larger association constant K than MB on bare/ODS-SOWG. The tendency is very interesting. We notice, however, that initial assumption of Langmuir model for binding process of dye–SOWG is a rather approximate one and it might not exactly reflect the true binding process. For the purpose of relative comparison of interaction of MB/NMB and bare/ODS-SOWG, such assumption is reasonable and simple.

3.3. Aggregation of MB and NMB in solution and on liquid–solid interface

The absorption spectra of MB and NMB highly depend on their concentration due to the monomer/dimer equilibrium as shown in Fig. 6. The inset in Fig. 6 clearly shows the monomer and dimer spectra after resolution by GRAMS/32. The corresponding dimer peak and monomer peak for MB in aqueous

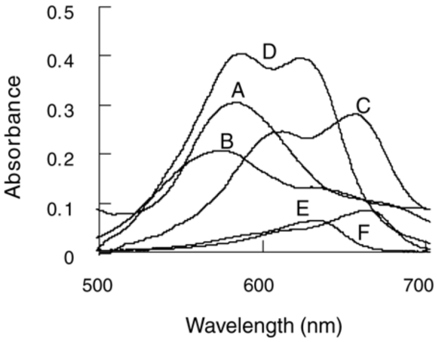

Fig. 7. Comparison of UV–visible spectra and absorption spectra (on bare/ODS-SOWG with a static cell) of MB, NMB: (A) MB on bare SOWG; (B) NMB on bare SOWG; (C) MB on ODS-SOWG; (D) NMB on ODS-SOWG; (E) NMB on UV–visible; (F) MB on UV–visible.

solution are at 604 and 664 nm, respectively. Similarly, NMB in aqueous solution shows its dimer peak at 588 nm and monomer peak at 632 nm. Fig. 6 also indicates that dimer peak intensity of MB in aqueous solution increases with increasing MB concentration. This means that it is difficult to observe dimer peak at low MB concentration in solution phase, owing to low sensitivity of UV–visible spectrophotometry. Fig. 7 shows the comparison of SOWG spectra and UV–visible spectra for MB and NMB. In Fig. 7, MB on ODS-SOWG has its monomer peak at 659 nm and dimer peak at 608 nm with GRAMS/32. For NMB on ODS-SOWG, it clearly indicates its corresponding monomer peak at 635 nm and dimer peak at 588 nm. These results are close to those obtained by Lee and Sung [37]. Moreover, one found that the ratio between the intensity of dimer peak and monomer peak for MB and NMB on ODS-SOWG increases very fast with increasing aggregation time, as shown in Fig. 7. One has also noticed that intensities of both dimer and monomer for MB and NMB at the same concentrations are much stronger than those obtained by UV–visible spectrophotometry. Therefore, SOWG is a very powerful technique for the study of adsorption of dye or other species in various conforms (e.g. monomer, dimer) at the liquid–solid interface, due to its higher sensitivity over conventional UV–visible spectrophotometry.

3.4. Effect of ionic strength on absorption of dye on SOWG surface

As one knows that adsorbates, at different modes like TE (transverse electric) and TM (transverse magnetic), will have different absorbance. In the present work, the effects of ionic strength on absorption of NMB on different SOWG surface (bare surface and ODS surface) were studied. As we can see from Fig. 8A and B, it seems that the higher the ionic strength of NaCl, the lower the absorbance of NMB measured by SOWG. This phenomenon is more obvious for the case of NMB adsorbed on bare SOWG surface. The possible reason for the above results is that introduce of counter-ion Cl^-, decreased the interaction NMB and SOWG surface.

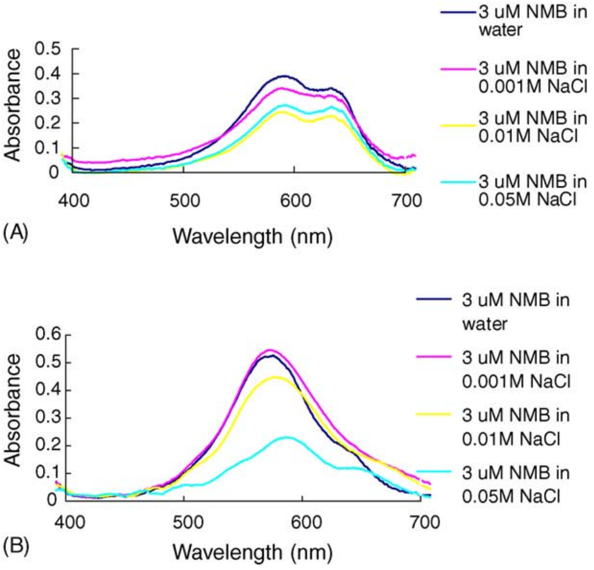

Fig. 8. Effect of ionic strength on absorption spectra: (A) NMB on ODS at TM mode; (B) NMB on bare plate at TM mode.

4. Conclusions

The adsorption characteristics of MB and NMB on both bare SOWG and ODS-SOWG show that both MB and NMB on ODS-SOWG distinctly displayed their corresponding monomer peaks and dimer peaks, which are more obvious than those observed from UV–visible spectra. Moreover, the ratio between the intensity of dimer peak and monomer peak of MB and NMB on ODS-SOWG increases with aggregation time. The SOWG technique is specifically effective in detecting the sample of low concentration. The ionic strength considerably affects the adsorption of dye like NMB and MB on SOWG surface.

Binding energy analysis of MB and NMB on bare SOWG and ODS-SOWG, based on molecular mechanics calculation showed that the binding energy for both MB and NMB on bare SOWG is larger than that on ODS-SOWG due to decrease of adsorption sites of glass surface, after the ODS modification which increases hydrophobicity of the glass surface. The difference in the binding energy for MB and for NMB on both bare SOWG and ODS-SOWG can be ascribed to the difference in their molecular structures.

Binding rate constant analysis showed that both MB and NMB on bare SOWG demonstrates larger association constants than those on ODS-SOWG, based on adsorption dynamics with Langmuir isotherm assumption. Results obtained show that the higher the binding energy, the larger the association constant *K*, except MB on bare ODS. Furthermore, NMB on bare/ODS-SOWG with higher binding energy than MB on bare/ODS-SOWG, gives larger association constant *K* than MB on bare/ODS-SOWG.

References

[1] C.M. Ruan, F. Yang, J.S. Xu, C.H. Lei, J.Q. Deng, Electroanalysis 9 (1997) 1180.

[2] H. Liu, T. Ying, K. Sun, D. Qi, J. Electroanal. Chem. 417 (1996) 59.

[3] R.B.M. Koehorst, G.K. Boschloo, T.J. Savenije, A. Goossens, T.J. Schaafsma, J. Phys. Chem. B 104 (2000) 2371.

[4] K. Sayama, K. Hara, N. Mori, M. Satsuki, S. Suga, S. Tsukagoshi, Y. Abe, H. Sugihara, H. Arakawa, Chem. Commun. 2000 (2000) 1173.

[5] A. Ehret, L. Stuhl, M.T. Spitler, Electrochim. Acta 45 (2000) 4533.

[6] J.J.B. Nevado, J.R. Flores, C.G. Cabanillas, M.J.V. Llerena, A.C. Salcedo, Talanta 46 (1998) 933.

[7] T. Nagy, K. Pataki, G. Gunther, P. Fekete, G. Farago, B. Lady, PCT Int. Appl. WO 9942087 A2 (1999); Chem. Abstr. 131:175079.

[8] K. Itoh, A. Fujishima, J. Phys. Chem. 92 (1988) 7043.

[9] M.D. DeGrandpre, L.W. Burgess, P.L. White, D.S. Goldman, Anal. Chem. 62 (1990) 2012.

[10] K. Tsunoda, H. Itabashi, H. Akaiwa, Anal. Chim. Acta 299 (1995) 327.

[11] J.E. Midwinter, IEEE J. Quant. Electron. QE-7 (1971) 339.

[12] R.E. Dessy, Anal. Chem. 61 (1989) 1079A.

[13] R.A. Potyrailo, S.E. Hoobbs, G.M. Hieftje, Fresen. J. Anal. Chem. 362 (1998) 349.

[14] Z.M. Qi, N. Matsuda, A. Takats, K. Kato, J. Phys. Chem. B 107 (2003) 6873–6875.

[15] N. Matsuda, A. Takatsu, K. Kato, Y. Shigesato, Chem. Lett. 125 (1998).

[16] K. Kato, A. Takatsu, N. Matsuda, Y. Shigesato, Chem. Lett. 583 (1997).

[17] T. Yoshida, H. Asano, J.H. Santos, Z.M. Qi, L.X. Sun, A. Takatsu, K. Kato, N. Matsuda, Chem. Lett. 32 (2003) 270–271.

[18] N. Matsuda, J. Santos, A. Takatsu, K. Kato, Thin Solid Films 438/439 (2003) 403.

[19] J.H. Santos, N. Matsuda, Z. Qi, A. Takatsu, K. Kato, Anal. Sci. 19 (2003) 199.

[20] N. Matsuda, J. Zheng, D. Qing, A. Takatsu, K. Kato, Appl. Spectrosc. 57 (2003) 100.

[21] Z. Qi, N. Matsuda, J.H. Santos, A. Takatsu, K. Kato, Opt. Lett. 27 (2002) 689.

[22] Z. Qi, N. Matsuda, T. Yoshida, H. Asano, A. Takatsu, K. Kato, Opt. Lett. 27 (2002) 2001.

[23] Z. Qi, N. Matsuda, A. Takatsu, K. Kato, K. Itoh, Appl. Spectrosc. 56 (2002) 1222.

[24] Z. Qi, N. Matsuda, J.H. Santos, K. Itoh, A. Takatsu, K. Kato, Langmuir 19 (2003) 214.

[25] J.H. Santos, N. Matsuda, Z. Qi, A. Takatsu, K. Kato, IEICE Trans. Electron. E85-C (2002) 1275.

[26] J.H. Santos, N. Matsuda, Z. Qi, T. Yoshida, A. Takatsu, K. Kato, Surf. Interf. Anal. 35 (2003) 432.

[27] T. Yoshida, H. Asano, J. Santos, Z. Qi, L. Sun, A. Takatsu, K. Kato, N. Matsuda, IEICE Trans. Electron. J85-C (2002) 1070.

[28] L.X. Sun, A. Mahipal Reddy, N. Matsuda1, A. Takatsu, K. Kato, T. Okada, Anal. Chim. Acta 487 (2003) 109–116.

[29] D.G. Kingston, B.B. Gerhart, J. Chromatogr. 116 (1976) 182.

[30] Oxford Molecular Ltd. http://www.xomol.com/; CAChe^{TM} Reference Version 3.9, CAChe Scientific Computer-Aided Chemistry from the Oxford Molecular Group.

[31] Fujitsu, Ltd. http://www.cache.fujitsu.com/.

[32] Y. Ebara, K. Itakura, Y. Okhata, Langmuir 12 (1996) 5165.

[33] L.X. Sun, T. Okada, J. Membrane Sci. 180 (2001) 213.

[34] J. Sagiv, J. Am. Chem. Soc. 102 (1980) 92.

[35] O. Askin Inel, A. Turk, J. Chem. 20 (1996) 276.

[36] N. Haimour, S.A. Sayed, Dirasat: Nat. Eng. Sci. 24 (1997) 215.

[37] C. Lee, Y.W.J.W. Sung, Park, J. Phys. Chem. 103 (1999) 893.